RevMexAA (Serie de Conferencias), **37**, 156–159 (2009)

A DESIGN OF AN ACOUSTO-OPTICAL SPECTROMETER

G. Herrera-Martínez,[1] A. Luna,[1] L. Carrasco,[1] A. Shcherbakov,[1] D. Sánchez,[1] E. Mendoza,[1] and F. Renero[1]

RESUMEN

La radioespectroscopía se ha convertido en una herramienta fundamental para estudiar objetos astronómicos en la banda de las microondas. Por lo tanto, es necesario el diseño y construcción de instrumentos con alta resolución espectral, bajo consumo de potencia y dimensiones lo más compactas posibles que hagan fácil su manejo y transporte. Aquí presentamos el diseño y pruebas de un espectrómetro acusto-óptico para uso en radioastronomía solar y para el estudio de la variabilidad de máseres cósmicos con una antena de 5 metros de diámetro (RT5) que se esta reinstalando en Sierra Negra. Mostramos las primeras evaluaciones del desempeño de los componentes y el ensamble de laboratorio.

ABSTRACT

The radio spectroscopy has became a fundamental tool to study astronomical objets at the microwave band. Therefore, the design and construction of instruments with high spectral resolution, low power consumption and compact size for easy handle and transport are necessary. Here we present the design and the tests of an acousto-optical spectrometer for use in solar radio astronomy and for variability studies of cosmic masers sources with a 5 meter antenna (RT5) which is being reinstalled at the Sierra Negra site. We present the first evaluations of the performance of the components and the laboratory assembly.

Key Words: Spectrometers — Acousto optics — Instrumentation

1. INTRODUCTION

The reinstallation of a 5 m dish radio telescope give us the oportunity to explore alternatives for spectrometer techniques. Three spectrometers types are common in radio astronomy: filter-bank, autocorrelator and acousto-optic. The filter-bank-type sprectrometers have several limitations: the maintenance and calibration required for every channel, and the fixed channel width. The autocorrellation-type is limited mainly by the power consumption and bandwidth because of current computer speed. The acousto-optical spectrometer (AOS) has been extensively used in radio astronomy, since Lambert described its principle (Lambert 1962). They are an efficient option for satellite telescopes (Klumb et al. 1994), due to the low power consumption and compact size which make easy to handle and transport.

Our main interest is the study of different astronomical objects at the millimeter band (~ 43 GHz). Figure 1 shows, for some of such objets, the required resolution and bandwidth. The plot shows that AOS is very well positioned for stellar formation and interstellar medium studies at these frequencies.

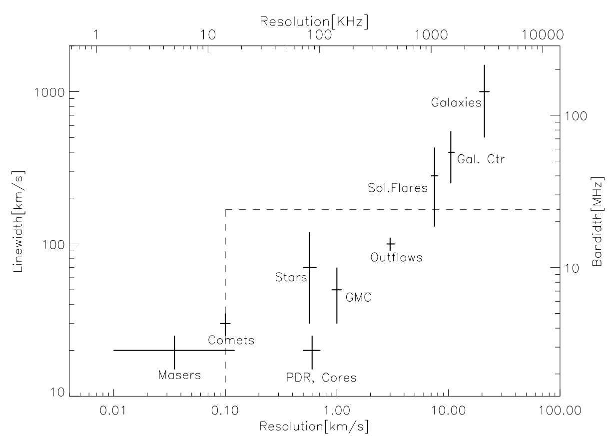

Fig. 1. Spectrometer bandwidth and spectral resolution at 43 GHz. The plot, adapted from (Harris 2002), shows the required velocities and frequencies for typical sources. The dashed line indicates the region of spectral resolution and bandwidth for this spectrometer according to the evaluation shown in § 3.

The principle of performance is as follows: the intermediate frequency (IF) of an heterodyne receiver of a radio telescope is injected into a piezo-electric transducer that mechanically modulate a Bragg cell illuminated by a collimated light beam. This Bragg cell, also known as Acousto-Optical Deflector (AOD), is an acusto-optical crystal of TeO_2 which deflects a laser light beam as a function of the injected IF. The TeO_2 crystal is known for its acousto-optical properties (Uchida & Kiizeki 1973).

[1] Instituto Nacional de Astrofísica Óptica y Electrónica, Mexico (gherrera@inaoep.mx).

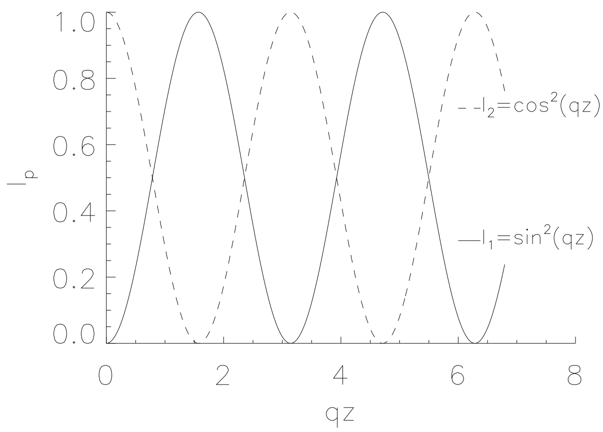

Fig. 2. Light intensity distribution in the Bragg regime, where the interaction lenght is large, this regime provides an oportunity of realizing 100% of light scattering.

The propagation of the acoustic wave through the photo-elastic medium produces traveling periodic variations in the refractive index of this medium. The diffraction pattern depends essentially on the length L of the interaction zone between the light beam and the acoustic waves. So the regimes of diffraction have two limiting cases, corresponding to a short and a large lengths of interaction. The Bragg diffraction regime, that we use, occurs with a large L. In this case the dynamic acoustic grating is rather thick. So, during the analysis of the diffraction process, one has to take into account the phase relations between waves of different orders. Such regime can be realized only when the angle of incident light θ_B on a thick acoustic grating meets the Bragg condition

$$\sin\theta_B = \frac{\lambda}{2n\Lambda};$$

and

$$Q = \frac{\lambda L}{\Lambda^2} \gg 1.$$

Here, Q is the Klein-Cook paramter (Klein & Cook 1967), λ is the laser wavelength, n is the refraction index of the crystal and Λ is the acoustic wavelength. The light intensity in orders of scattering is shown in Figure 2, where

$$q = \pi(\lambda\cos\theta)^{-1}\sqrt{2M_2PS^{-1}};$$

M_2 is the acousto-optic figure of merit, and P/S is the acoustic power density. It is desirable to perform the Bragg regime since it reaches 100% efficiency of light scattering.

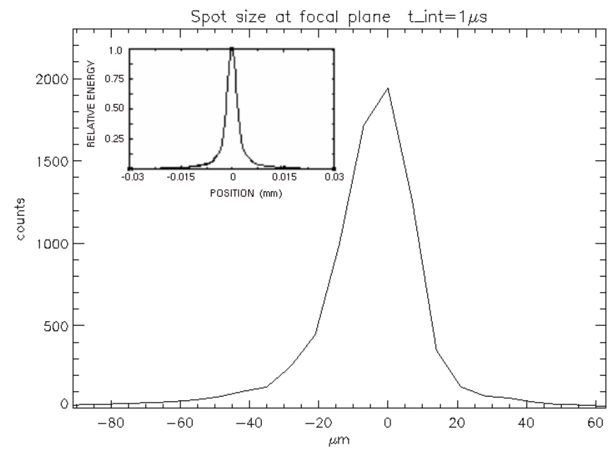

Fig. 3. Comparison of the simulated spot size (subframe) with OSLO EDU 6.4.5 and a measurement of a large format lenses system of Edmund optics with $FWHM \simeq 24$ μm.

TABLE 1

SPOT SIZE EVALUATION

Stock number	Lens diam. (mm)	Focal distance (mm)	Spot diam. (μm)	Airy diam. (μm)
Edmund u32-925	40	200	6.5	16
Melles Griot lao-631	50	250	6.5	18
Thorlabs AC508-250-A1	50.8	250	6.4	14
Newport PAC088	50.8	250	6.4	14

2. FOCUSING SYSTEM AND SPOT SIZE EVALUATION

We have theoretically investigated the potential size of an individual resolvable spot inherent in various lens sets in a view of optical matching the AOD aperture (about 40 mm) with a pair of the CCD-camera pixels (about 14 μm). For this purpose, we have used the OSLO EDU 6.4.5 ray tracing software and analyzed the spot size of more than 20 various types of lens sets. The result are given in Table 1, were it may be seen that we have obtained two potentially acceptable lens sets from Thorlabs and Newport with a same spot size of about 14 μm and a focal distance of 250 mm. They both are potentially suitable for the goals of the AOS under construction.

Figure 3 shows the spot size measured in the focal plane of the focus lens system. This size defines the

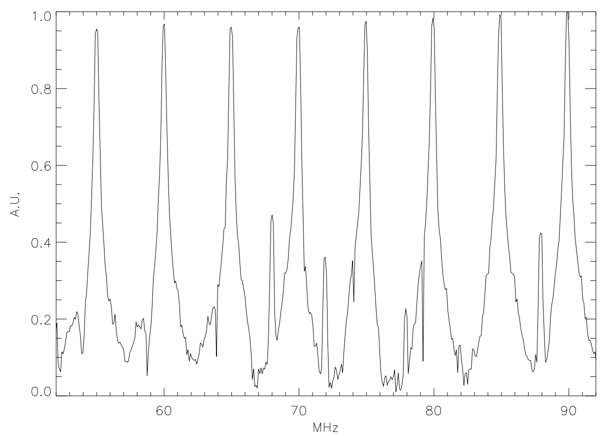

Fig. 4. Injected signal of the AOD driver signal sweeped from 55 to 90 MHz, with a 5 MHz step.

spectrometer band resolution. For a Edmund Optics focusing lens system a spot size of 4 pixels at FWHM was reached ($\sim$ 28 microns).

3. AOD EVALUATION AND PERFORMANCE

The AOD, manufactured by *Molecular Technology GmbH*, consists of a driver, which manages the injected signal to the transducer, and the optical block, where the piezoelectric transducer, the crystal and the absorber for the acoustic wave, are placed.

First, we perform computations for the spectral resolution (δf) and the bandwidth (ΔF) intrinsic to our AOD. With a large optical window and a low sound velocity into crystal we can improve the resoution. The data sheet of AOD specifics the sound velocity in the crystal, $650\,\mathrm{km\ s^{-1}}$, and the optical window, 40×10 mm. A linear CCD array with 3000 pixels (#CCD) and a pixel size of $14 \times 200\,\mu$m was used. We obtain

$$\delta f = \frac{V_{\rm sound}}{L_{\rm crystal}} = \frac{650\mathrm{ms}^{-1}}{40\mathrm{mm}} = 16.24\,\mathrm{KHz}\,,$$

and the bandwidth

$$\Delta F = \frac{\delta f\#\mathrm{CCD}}{2} = 24.3\,\mathrm{MHz}\,.$$

In terms of the velocity at the 43 GHz frequency ($\lambda_0 = 7$mm) the results are $0.1\,\mathrm{km\ s^{-1}}$ and $168\,\mathrm{km\ s^{-1}}$ respectively (dashed line of Figure 1).

In the practice, we first evaluate the dispersion angle(ϕ) of the AOD at different frequencies using the aproximation:

$$\tan\phi = \frac{f\lambda}{V_{\rm sound}};$$

TABLE 2

EVALUATION OF THE DIFFRACTION ANGLES

Frequency (MHz)	Distance on screen (mm)	Expected value (°)	Measured value (°)
55	79	3.07	3.08 ± 0.03
60	86	3.34	3.35 ± 0.03
65	93	3.62	3.62 ± 0.03
70	101	3.90	3.93 ± 0.03
75	107	4.18	4.16 ± 0.03
80	114	4.45	4.43 ± 0.03
85	122	4.73	4.74 ± 0.03
90	128	5.01	4.98 ± 0.03

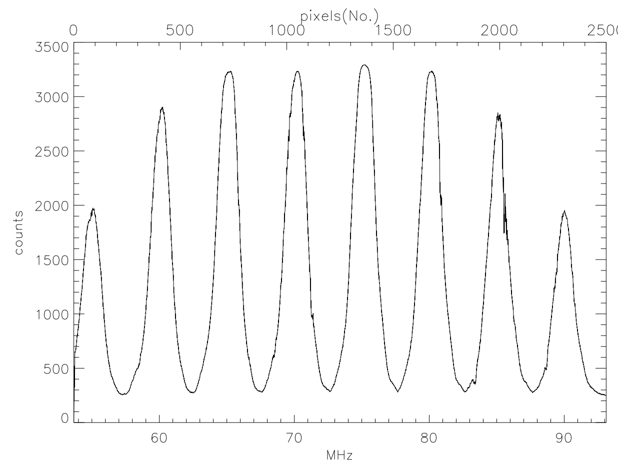

Fig. 5. Qualitative spectrum of the AOS without focusing optics and a CCD integration time of 1μs. For frequency calibration the better fit was linear, with this, the bandwidth by a pair of pixels are ~ 32 KHz.

where f is the frequency of the acoustic wave, λ is the laser wavelength and $V_{\rm sound}$ is the sound velocity in the crystal.

A He-Ne laser module of 633nm@12mW with linear polarization was used to illuminate orthogonally the AOD window. The projection of the diffracted beam was measured in a screen at 1470 mm away from the output of the cell. A signal frequency sweeped in frequency from 55 MHz to 90 MHz with a 5 MHz step was used. The results are shown in Figure 4.

Measurements of the diffraction angle are listed in Table 2. The percentage error is less than 10% of the expected value. The scanning angle in the air for all the bandwidth is $2.2° \pm 0.03$, in good agreement with the data sheet (2.25°). The AOD was

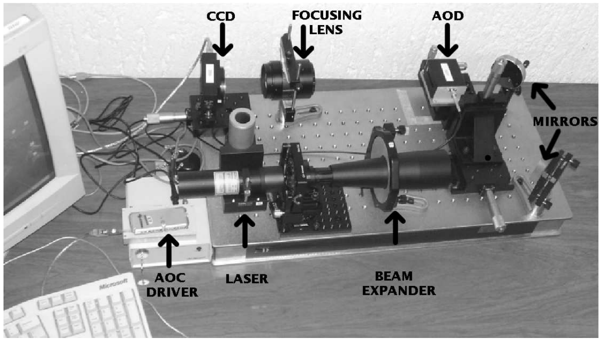

Fig. 6. Actual assembly of AOS, all the components are mounted in a optical bench of 1×2 ft, the expansion of laser beam is doing by a galilean telescope with magnification of 15x.

constructed so that the incident light beam should be orthogonal to the input optical plane of the cell, and the light polarization plane should be parallel to the base of optical block. This construction provides the maximum scanning angle value.

We can see that the range of diffraction angle is appropiate for our purposes. To get a better frequency resolution we need a focusing lens with a good spot size at the focal plane.

4. WORK IN PROGRESS

To get the resolution closer to the desired one of 16 KHz it is necessary to expand and collimate the laser beam to fully illuminate the optical window of the AOD. Our first approximation to expand the beam is using a Galilean telescope with a magnification of $15\times$ and a laser diode module with beam diameter of $1.5 \times 5.25@1/e^2$. We will analyze the use of a set of prisms to expand the laser beam. Software of the driver control of the AOD and the acquisition data software of the CCD camera will be improved to do it more efficient and obtain a faster performance.

In Figure 5, the measurement of the intensities at different angles of diffracted beam on the CCD camera without focusing optics are shown. For the frequency calibration a gaussian fit for every beam was made so we locate the pixel postion where the maximums are. Using least squares we calculate the better fit, there is a lineal relationship between the separation of the maximums and the deflection angle of the beam. With this, the spectral resolution in a pair of pixels is ~ 64 KHz. Furthermore we can see a surrounding shape like a function of the deflected angle. If we change the frequency of the acoustic wave, we will see how it varies the intensity of the deflected beam too.

The laboratory assembly is shown in Figure 6. Two mirrors are needed to bend the optical path due to the dimentions of the optical bench. Some additional mechanical parts have been made to get the best alignment of the optical path.

REFERENCES

Harris, A. I. 2002, in Proc. Far-IR, Sub-mm and Millimeter Detector Technology Workshop, ed. J. Wolf, J. Farhoomand, & C. R. McCreight, NASA CP-211408
Klein, R. W., & Cook, B. D. 1967, IEEE Trans. Sonics and Ultrasonics, 14, 123
Klumb, M., Frerick, J., Tolls, V., Schieder, R., & Winnewisser, G. F. 1994, Proc. SPIE, 2268, 305
Lambert, L. B. 1962, IRE Int. Conu. Rec., 6, 69
Scalise, E. 1999, ASSL, 241, 447
Schieder, R. T., et al. 2003, Proc. SPIE, 4855, 290
Shcherbakov, A., Luna, A., Ledeneva, Y., & Maximov, J. 2007, in Proc. XXII Annual Congress Soc. Mexicana Instrum.
Shcherbakov, A., Luna, A., & Sánchez, D. 2008, in Proc. XXIII Annual Congress Soc. Mexicana Instrum.
Uchida, N., & Kiizeki, N. 1962, Proc. Inst. Radio Elec. Electron. Engrs., 61, 1073